

USING A STANDARD SPECIMEN GEOMETRY FOR CRACK PROPAGATION UNDER PLAIN STRAIN CONDITIONS

J.M. Silva¹, V. Infante², F. Antunes³, F. Ferreira¹

¹ Departamento de Ciências Aeroespaciais,
Universidade da Beira Interior; 6201-001 Covilhã – Portugal
E-mail: jmas@ubi.pt

² Departamento de Engenharia Mecânica
Instituto Superior Técnico; 1049-001 Lisboa – Portugal
E-mail: virginia@dem.ist.utl.pt

³ Departamento de Engenharia Mecânica
FCTUC; 3030-788 Coimbra – Portugal
E-mail: fernando.ventura@dem.uc.pt

ABSTRACT

This work is a preliminary approach to evaluate the possibility of using a conventional M(T) specimen with lateral notches aiming at obtaining plane strain conditions required for certain type of phenomena concerning crack propagation. This type of specimen geometry can be advantageous since it allows the use of moderate component thicknesses with triaxial stress conditions in the most part of the crack propagation region.

Several computational simulations of fatigue cracks in an aluminium alloy were carried out by using commercial FEM codes. The influence of different types of variables was considered, namely the geometry of the lateral notches (circular or V shaped) and the thickness of the specimen. Stress intensity factor K was determined for several crack front positions to evaluate the effect of these geometrical features, as well as the influence of both stress fields and crack length in the fatigue behaviour of the material. Also, two stress triaxility parameters were used in order to confirm the stress state condition in the crack propagation region.

The conclusions of this preliminary study are encouraging concerning the possibility of using a reduced thickness MT specimen with a plane strain condition, which can be a useful experimental tool when considering the investigation of particular crack propagation mechanisms, such as those related with high temperature conditions.

KEY WORDS: M(T) specimen, triaxility parameters, stress intensity factor, fatigue

1. INTRODUCTION

Stress state is a main independent parameter with a notorious effect in fatigue crack growth under certain types of loading and environmental conditions. As an example, high temperature fatigue crack propagation in some types of materials, such as nickel base superalloys, is a complex phenomenon characterized by different damage micromechanisms, namely cyclic plastic deformation, oxidation and creep [1,2]. Depending on the conditions at the crack tip one of these mechanisms may be dominant and the propagation is either transgranular (cyclic plastic deformation), intergranular (oxidation or creep) or mixed. Stress state directly affects these distinct propagation modes: a plane stress state was found to promote transgranular propagation, whilst the triaxility associated to plane strain state promote diffusion mechanisms associated with time dependent propagation [3].

Plasticity induced crack closure (PICC) [4,5] is another phenomenon which can be greatly influenced by the

stress state condition. There is a general agreement that plane stress state induces significantly larger levels of crack closure compared with those related to plane strain loading conditions. However, the intensity and even the existence of PICC under plane strain conditions are still controversial. From a theoretical point of view, the main problem is to visualise the additional volume of material necessary to explain PICC, since out-of plane flow is not allowed under plane strain conditions, by definition. So, if a constant volume during deformation is taken into account, the assumption of an additional wedge is not reasonable [6,7]. A significant number of numerical studies focusing on PICC under plane strain conditions have been developed. However, their validation through a convenient experimental work is difficult due to the inexistence of a pure plane strain specimen geometry.

In fact, for experimental fatigue testing purposes, plane stress conditions are usually obtained by simply using thin specimens based on standard geometries. BS 6835

1988 [8] and ASTM 647-95a [9] indicate the use of CT, MT and bending specimens. By the other hand, when plane strain is intended to occur as a sole condition, specimens are required to have increased thicknesses which, in turn, does not eliminate possible surface effects and leads to more complex and expensive testing procedures. The inclusion of lateral notches on the specimens is a possible solution to overcome these limitations, allowing obtaining plane strain conditions in relatively thin specimens, which will be explored here.

Fatigue crack growth in specimens with lateral notches and under different loading conditions has been widely reported by several authors [10-15], but without aiming at obtaining plain strain conditions in all the positions of the crack front.

The analysis and optimization of pure plane strain specimens requires numerical parameters to quantify stress triaxiality. Several authors [16-20] used the triaxiality parameter Θ as defined by Eq. (1):

$$\Theta = \frac{\sigma_m}{\sigma_v} = \frac{\frac{1}{3}(\sigma_{xx} + \sigma_{yy} + \sigma_{zz})}{\frac{1}{\sqrt{2}}[(\sigma_{xx} - \sigma_{yy})^2 + (\sigma_{xx} - \sigma_{zz})^2 + (\sigma_{yy} - \sigma_{zz})^2]^{1/2}} \quad (1)$$

Θ is the ratio between the average hydrostatic stress and equivalent Von Mises stresses, and σ_{xx} , σ_{yy} and σ_{zz} are the stresses along x , y and z directions, respectively. Lemaitre [20] proposed another triaxiality parameter defined by Eq. (2):

$$R_v = \frac{2}{3}(1-\nu) + 3(1-2\nu)\left(\frac{\sigma_H}{\sigma_{eq}}\right)^2 \quad (2)$$

This triaxiality parameter is based in the ratio of the hydrostatic stress and equivalent Von Mises stresses, and for practical engineering problems its value is typically between 0 (pure shear) and 5 to 6 in the vicinity of very sharp notches.

A third possible triaxiality parameter h given by Eq. (3) can be derived from the general equilibrium stress equations for a cracked body:

$$h = \frac{\sigma_{zz}}{\nu(\sigma_{zz} + \sigma_{zz})} \quad (3)$$

where ν is the Poisson's ratio. h has the values of 1 and 0 for plane strain and plane stresses, respectively.

The main objective of this paper is to propose plane strain specimen geometry adequate for studies of high temperature fatigue crack growth and plasticity crack closure, among other phenomena. The effect of lateral notches on stress triaxiality is studied for different specimen geometries. Stable crack shapes are obtained and used to come to closed-form solutions for stress intensity factor.

2. NUMERICAL PROCEDURE

Fracture mechanics parameters and fatigue crack propagation were obtained from different numerical simulations based in two FEM codes: ABAQUS® v6.5 and ZENCRACK® v7.5. The first software was used to create the physical model and to obtain the visualization of the output parameters, whilst the latter was specifically oriented to generate a proper finite element mesh in the vicinity of the crack using pre-defined crack blocks. Stress intensity factor K for different crack front positions was also determined from ZENCRACK® based on the relative displacements derived from an orthogonal set of axes at each crack front node.

The geometry of the Middle-Tension, M(T), specimen considered for the FEM analysis is presented in Figure 1. All simulations were based in the same general dimensions of this specimen: 200×50×10mm (length×width×thickness). The geometric features of the lateral notches are indicated in Table 1.

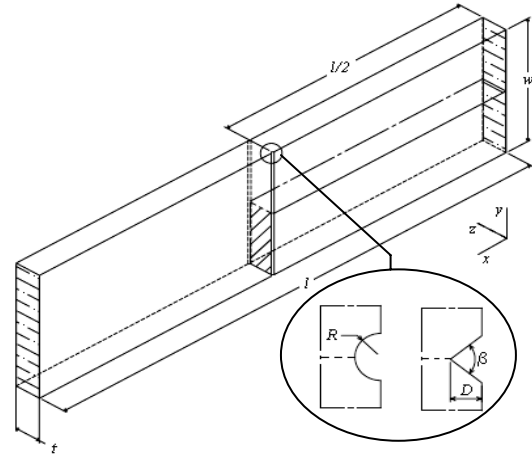


Figure 1 – Geometry of the M(T) specimen (D – Depth, R – Radius, β – Angle)

The material used in this study is a high specific strength structural aluminum alloy (6082-T6) with homogeneous and isotropic characteristics, and its main mechanical properties are indicated in Table 2.

Figure 2 shows the loading and boundary conditions applied to the specimen. A maximum distributed load of 5000 N was considered for all cases, which corresponds to a maximum nominal stress of 10 MPa. Due to symmetry conditions of both the specimen and loading, only 1/4 of the specimen was assumed in the analysis.

Symmetry boundary conditions were also applied to the crack plane points, excluding those of the crack propagation zone which had no constraints to allow for the crack opening. Additionally, other displacement constraints were considered as follows:

1. x direction restriction in the vertical plane of symmetry (except for the crack points);
2. y direction restriction in the horizontal plane of symmetry;
3. z direction restriction in the remaining surfaces by using 2 degrees of freedom (x and y directions).

Table 1 – Notch dimensions: R , β , D

Dimensions [mm]		
R	β	D
0.5	-	-
0.75	-	-
1	-	-
0.75	-	0.5
1	-	0.5
-	30°	0.5
-	60°	0.5
-	90°	0.5
-	120°	0.5

Table 2 – Mechanical properties of aluminum alloy 6082-T6

Yield stress	307±2.7 MPa
UTS	330±2.5 MPa
Young modulus	74×10 ³ MPa
Poisson coefficient	0.33
Vickers hardness	100 kgf/mm ²

The finite element mesh was implemented using isoparametric elements with 20 nodes and full integration. Crack tip elements must incorporate a singularity in their formulation, which can be correctly represented by using a collapsed isoparametric “quarter-point” element. Finally, standard crack-blocks from ZENCRACK[®] were used to create the mesh of elements in the crack front. All of these blocks have a spider web shape allowing for a smooth transition between the crack front region, where a higher mesh refinement is recommended, and the remote regions of the specimen.

A special caution was driven towards the number of contours in each crack-block for K determination purposes. In fact, the number of contours must be high enough to allow for the convergence of the value of the stress intensity factor in a particular position in the crack front. In this case, it was found that the use of crack-blocks with 6 contours was enough to accomplish this requirement.

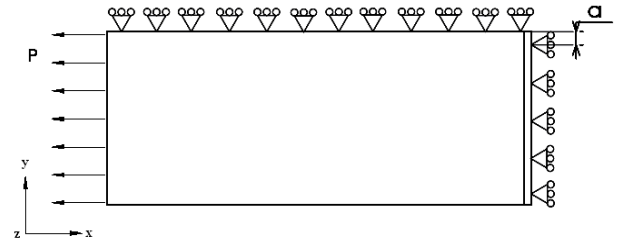


Figure 2 – Loading and boundary conditions.

3. RESULTS AND DISCUSSION

As previously mentioned, one major goal of this work is to evaluate the effect of different types of notches (dimensions and geometries) on the value of the stress intensity factor for distinct crack front positions in a M(T) specimen. Figure 3 shows the distribution of K considering four types of notches: V-notch (with $\beta=30^\circ$ or $\beta=60^\circ$), circular (with $R=0.5\text{mm}$) and elliptical ($R=0.75\text{mm}$ and $R'=0.5\text{mm}$). In all cases, a 10mm width specimen with a crack of 1mm was considered.

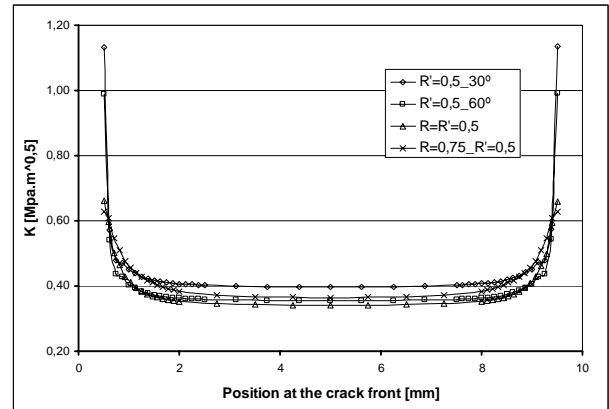


Figure 3 – Variation of the stress intensity factor K for different positions at crack fronts with 1mm.

From this figure, it is clear that the steep stress gradients induced by all notches results in a substantial increasing of the stress intensity values near the surface of the specimen, i.e., in the vicinity of the notch root. However, this effect is more evident for the case of the V-notches, particularly with $\beta=30^\circ$, since this geometry leads to the highest stress concentration factors. On the opposite side, the smallest values of K were obtained for the circular or elliptical notches, which means that these geometries are less severe in terms of stress distribution.

The triaxility effect induced by notches was evaluated for two distinct situations: with and without crack. Stress triaxility was quantified using the parameters defined by Equations (1) and (3), namely Θ and h . All situations were based in two types of geometry of notches: V-notch and circular.

Figure 4 illustrates the variation of both parameters h and Θ along half width of a non-cracked M(T) specimen with two circular lateral notches ($R=0.5\text{mm}$).

As one can see, these two parameters show a similar behaviour, which is characterized by a significant increase of its values towards the surface of the specimen and near the root of the notch. In this region, $h \rightarrow 1$ confirming the influence of the notch for the occurrence of strain plane conditions.

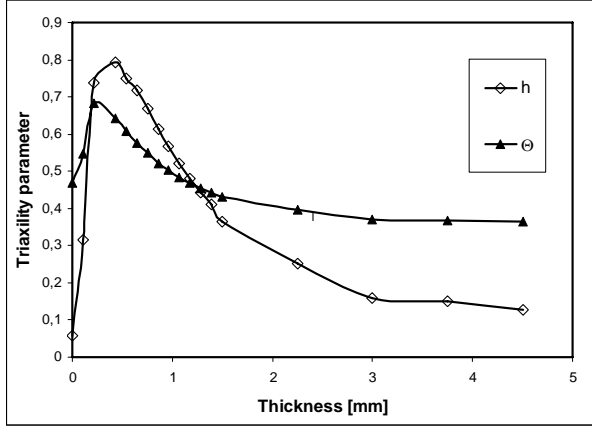


Figure 4 – Variation of parameters h and Θ along half width of a non-cracked M(T) specimen with two circular lateral notches ($R=0.5\text{mm}$)

Since h and Θ evince similar qualitative behaviours regardless the type of notch geometry, all subsequent results will be based only in the analysis of the variation of h along the width of the specimen.

Figures 5 and 6 present the profile of the stress triaxiality parameter h considering the effect of a circular notch with different radius ($R=0.5\text{mm}$, $R=0.75\text{mm}$ and $R=1\text{mm}$) and a V-notch with variable angle ($\beta=15^\circ$, $\beta=30^\circ$, $\beta=45^\circ$ and $\beta=60^\circ$), respectively. From these figures, it is clear that there is a peak of the stress triaxiality parameter for both types of notch geometries near the root of the notch. At the same time, the reduction of either the notch radius (circular notch) or β angle (V-notch) results in a considerable increase of h , which assumes a value close to unity in the case of sharper V-notches (i.e., with smaller β). This means that this type of notch geometry is more effective for obtaining triaxiality stress conditions near the surface of the specimen. However, it is interesting to note that the use of circular notches leads to a larger extension of the zone of influence of the notch, which means higher values of h towards the interior of the specimen. This effect is particularly visible in the case of the circular notch with $R=1\text{mm}$.

The thickness of the specimen is another important variable with a notorious effect in the triaxiality of stresses. Figure 7 shows the variation of the triaxiality parameter h considering the effect of the alteration of the thickness for a specimen with a circular notch geometry ($R=1\text{mm}$). The results clearly show that thinner specimens have a larger region under triaxiality stress conditions, which can be concluded from the smaller variation of h from the notch root towards the

interior of the specimen. Thus, for experimental testing of components under plane strain conditions, it is important to choose the right combination between the type of notch to be used (in terms of geometry and dimensions) and the specimen's thickness.

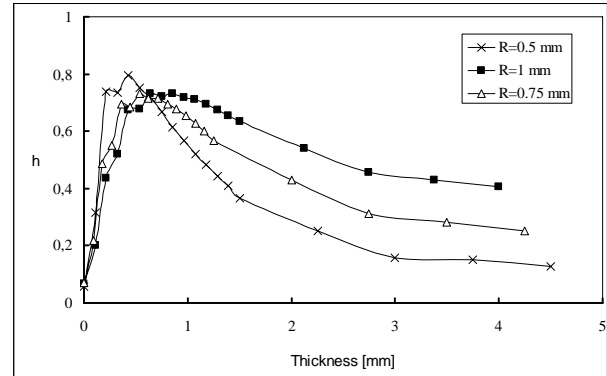


Figure 5 – Variation of triaxiality parameter h considering the effect of a circular notch with different radius ($R=0.5\text{mm}$, $R=0.75\text{mm}$ and $R=1\text{mm}$).

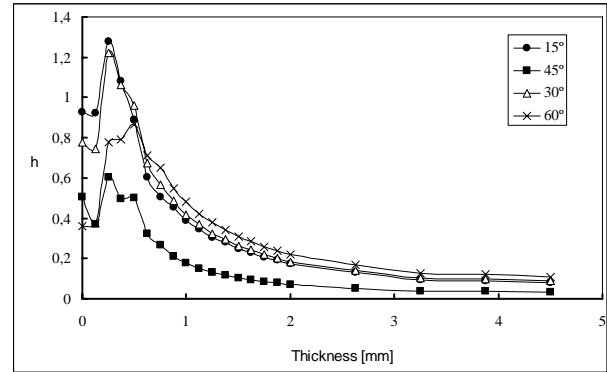


Figure 6 – Variation of triaxiality parameter h considering the effect of a V-notch with variable angle ($\beta=15^\circ$, $\beta=30^\circ$, $\beta=45^\circ$ and $\beta=60^\circ$).

As discussed in Chapter 1, the possible use of a thin specimen under plane strain conditions is determinant for the experimental investigation of certain types of phenomena, such as high temperature crack propagation. Consequently, the evaluation of triaxiality effects due to presence of notches in a cracked specimen is of utmost importance.

Figure 8 illustrates the variation of the triaxiality parameter h for two types of geometries of notches: circular ($R=0.5\text{mm}$) and V shaped ($\beta=60^\circ$, $\beta=90^\circ$ and $\beta=120^\circ$). For comparative purposes, the profile of h for a specimen without lateral notches is also indicated. All the results were obtained for a crack extension of 5mm.

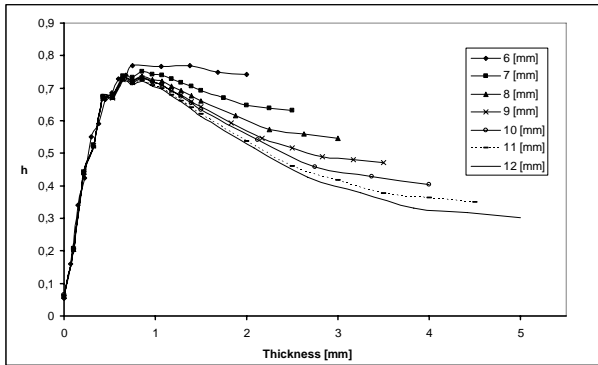


Figure 7 – Variation of the triaxility parameter h considering the effect of the alteration of the thickness for a specimen with a circular notch geometry ($R=1\text{mm}$)

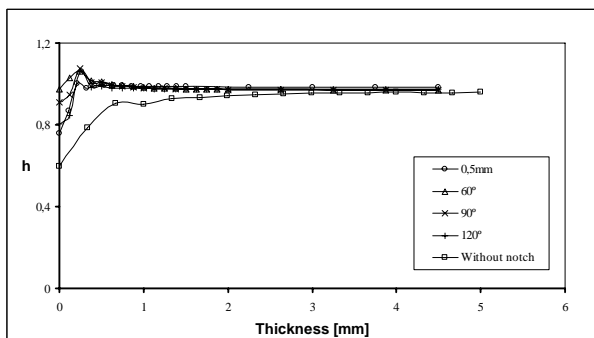


Figure 8 – Variation of the triaxility parameter h for two types of geometries of notches: circular ($R=0.5\text{mm}$) and V shaped ($\beta=60^\circ$, $\beta=90^\circ$ and $\beta=120^\circ$).

The observation of these curves allow to conclude that there is a significant effect of the notches, regardless its geometry, for obtaining a triaxility state near the surface of the specimen. Nevertheless, the presence of a crack front by itself is a promoting factor for the existence of high values of triaxility in almost all the thickness of the specimen, even without the presence of any type of lateral notches. Additionally, the triaxility effect of the V-notches is slightly higher for those crack front positions near the surface of the specimen. However, both types of geometries of notches (circular and V shaped) have very similar h values regarding the rest of the specimen's thickness. Considering the fact that a perfect sharpened notch is difficult to obtain in real conditions, these results show that the use of a circular notch is a good trade-off between the easiness of fabrication of the specimen and the existence of plane strain conditions in all the positions of the crack front, which is the main goal of this work.

4. CONCLUSIONS

This preliminary work is intended to evaluate the possible use of a standard M(T) specimen geometry under plane strain conditions to investigate certain types of phenomena, such as high temperature crack propagation. From the computational results, some main conclusions can be highlighted:

- There is a clear effect of the stress concentration region induced by the presence of lateral notches, regardless its geometry. This effect results in a substantial increase of the stress intensity factor near the notch root;
- V-shaped notches have a stronger triaxility effect when compared with circular notches, which is reflected in higher values of the triaxility parameters (Θ and h) in positions near the surface of the specimen. However, the use of circular notches leads to higher values of the triaxility parameters in the interior of the specimen;
- The thickness of the specimen has a strong influence in the variation of the triaxility parameters. Thinner specimens with lateral notches are characterized by having a nearly constant value of the triaxility parameters from the surface positions towards the interior of the specimen;
- The use of either circular or V-shaped lateral notches in a standard M(T) specimen with a fatigue crack allows for its propagation under plain strain conditions in all positions of the crack front.

5. RERERENCES

- [1] G.A. Webster and R.A. Ainsworth; “*High Temperature Component Life Assessment*”; Ed. Chapman & Hall, UK; 1994.
- [2] H. Ghonem, T. Nicholas and A. Pineau; “*Elevated Temperature Fatigue Crack Growth in Alloy 718- Part II: Effects of Environmental and Material Variables*”; Fat. and Fract. of Eng. Materials and Structures, 16, 6; Elsevier; 1993; 577-590.
- [3] F.V. Antunes, J.A.M. Ferreira, C.M. Branco e J. Byrne; “*Influence of stress state on high temperature fatigue crack growth in Inconel 718*”; Fatigue and Fracture of Eng. Materials and Structures 24; Elsevier; 2001; 127-135.
- [4] Elber W.; “*Fatigue crack closure under cyclic tension*”; Eng. Fracture Mechanics, 2; 1970; 37-45.
- [5] Antunes FV, Rodrigues DM.; “*Numerical simulation of plasticity induced crack closure: Identification and discussion of parameters*”; Engng Fracture Mech, 75; 2008; 3101–3120.
- [6] R.C. McClung, B.H. Thacker, S. Roy; “*Finite element visualization of fatigue crack closure in plane stress and plane strain*”, Int. J. Fracture, 50; 1991; 27-49.
- [7] Riemelmoser, F.O. and Pippan, R.; “*Plasticity-Induced Crack Closure Under Plane Strain Conditions in Terms of Dislocation Arrangement*”; Proc. of 6th International Fatigue Congress, Berlin, Germany; Ed. by G. Lütjering and H. Nowack; 6-10 May; 1996.
- [8] BS 6835-1 : 1998 – “*Method for the determination of the rate of fatigue crack growth in metallic materials*”; BSI; London, UK; 1998.
- [9] ASTM 647 - 95 a – “*Standard test method for measurement of fatigue crack growth rates*”; ASTM International; West Conshohocken, USA; 1995.
- [10] E .N. Brown, R. S. White and N. R. Sottos; “*Fatigue crack propagation in microcapsule toughened*

- epoxi*"; Journal of Materials Science, 41, 19; 2006; 6266-6273;
- [11] G. Lin, A. Cornec and K.-H. Schawalbe; "*Three-dimensional finite element simulation of crack extension in aluminium alloy 2024FC*"; Fatigue and Fracture of Engineering Materials and Structures, 21; 1998; 1159-1173.
- [12] A. Carpinteri, R. Brighenti and S. Vantadori; "*Surface cracks in notched round bars under cyclic tension and bending*"; International Journal of Fatigue, 28; 2006; 251-260;
- [13] Lin XB, Smith RA.; "*Shape evolution of surface cracks in fatigued round bars with a semicircular circumferential notch*"; International Journal of Fatigue, 21; 1999; 965-973.
- [14] Lin XB, Smith RA.; "*Fatigue growth simulation for cracks in notched and unnotched round bars*"; International Journal of Mechanical Sciences, 40; 1998; 405-419.
- [15] A. Carpinteri, R. Brighenti and S. Vantadori; "*Circumferentially notched pipe with an external surface crack under complex loading*"; International Journal of Mechanical Sciences, 45; 2005; 1929-1947
- [16] G. Mirone; "*Role of stress triaxiality in elastoplastic characterization and ductile failure prediction*"; Engineering Fracture Mechanics, 74; 2007; 1203-1221
- [17] W. Shen, L.H. Peng, C.Y. Tang.; "*An anisotropic damage-based plastic yield criterion and its application to analysis of metal forming process*"; International Journal of Mechanical Science, 47; 2005; 1897-1922;
- [18] S. Chandrakanth and P. C. Pandey; "*An Isotropic Damage Model for Ductile Material*"; Engineering Fracture Mechanics, 50, 4; 1995; 457-465;
- [19] B. S. Henry and A. R. Luxmoore; "*The Stress Triaxiality Constraint and the Q -Value as a Ductile Fracture Parameter*"; Engineering Fracture Mechanics, 57, 4; 1997; 375-390;
- [20] Lemaitre J.; "*A Course on Damage Mechanics*"; Springer; New York; 1996.